

# New $\text{Ni}_5\text{Al}_3$ Underlayer for Longitudinal Magnetic Recording Media

Yu-Nu Hsu, David N. Lambeth, *Fellow, IEEE*, and David E. Laughlin

**Abstract**—We describe a new  $\text{Ni}_5\text{Al}_3$  underlayer for high-density longitudinal magnetic recording. The  $\text{Ni}_5\text{Al}_3$  underlayer has the FCC derivative  $\text{Ga}_3\text{Pt}_5$  structure. The  $\text{Ni}_5\text{Al}_3$  (221) plane has good lattice match with the  $\text{CoCrPt}$  (10  $\bar{1}$  0) plane. In addition, unlike the  $\text{NiAl}$  (112) plane, the  $\text{Ni}_5\text{Al}_3$  (221) plane has the lowest surface energy. Hence, the  $\text{Ni}_5\text{Al}_3$  thin film has a strong (221) texture and can induce  $\text{CoCrPt}$  (10  $\bar{1}$  0) texture. The microstructure and magnetic properties of the  $\text{CoCrPt}$ - $\text{Ni}_5\text{Al}_3$  thin films are reported and discussed.

**Index Terms**—Co alloy magnetic film, epitaxial growth, lattice match, longitudinal magnetic recording thin film,  $\text{NiAl}$  underlayer,  $\text{Ni}_5\text{Al}_3$  underlayer.

## I. INTRODUCTION

TO ACHIEVE higher longitudinal magnetic recording density, the transition length of the media has to be reduced. This can be achieved by increasing the media coercivity. In order to achieve high coercivity and high  $k_u$ , we must obtain  $\text{CoCrPt}$  grains of such crystalline perfection that the  $\text{CoCrPt}$  magnetocrystalline anisotropy is maximized and not compromised by lattice strain and defects. This can be achieved by obtaining a strong  $\text{CoCrPt}$  crystallographic texture with the easy axes aligned in the thin film plane and with a minimum amount of misfit between the magnetic film and the underlayer.

The texture and grain size of the  $\text{CoCrPt}$  magnetic layer can be controlled by using underlayers. The currently popular  $\text{NiAl}$  (112) underlayer can be used to induce the  $\text{CoCrPt}$  (10  $\bar{1}$  0) texture [1] with  $c$  axis aligned in the thin film plane. However, the  $\text{NiAl}$  (112) plane is probably not the lowest surface-energy plane and therefore a strong  $\text{NiAl}$  (112) texture cannot be easily obtained. High-resolution TEM has shown that a  $\text{NiAl}$  (112) texture is not usually obtained unless the  $\text{NiAl}$  underlayer obtained by our deposition system is thicker than about 80 nm [2]. As a result, the  $\text{NiAl}$  (112) texture does not usually induce strong  $\text{CoCrPt}$  (10  $\bar{1}$  0) texture. In this paper, we introduce a new underlayer, with composition  $\text{Ni}_5\text{Al}_3$  having a different crystal structure than the B2  $\text{NiAl}$ . This new underlayer could induce a strong  $\text{CoCrPt}$  (10  $\bar{1}$  0) texture and small  $\text{CrCrPt}$  grains.

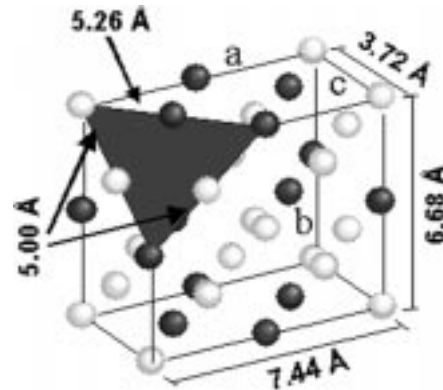


Fig. 1. Schematic of the  $\text{Ni}_5\text{Al}_3$  unit cell and the  $\text{Ni}_5\text{Al}_3$  (221) planes.

### A. $\text{Ni}_5\text{Al}_3$ Phase and Epitaxial Relationship With Co-Alloy Magnetic Layer

The single phase region of the  $\text{Ni}_5\text{Al}_3$  phase extends from about 64 at% to 68 at% of Ni below 700 °C [3]. Because the  $\text{Ni}_5\text{Al}_3$  phase is stable at a room temperature, it is easy to obtain this phase by thin film deposition.

$\text{Ni}_5\text{Al}_3$  has the  $\text{Ga}_3\text{Pt}_5$  structure, which is an FCC derivative structure with orthorhombic symmetry. The lattice parameters of the  $\text{Ni}_5\text{Al}_3$  phase are  $a = 7.44$  Å,  $b = 6.68$  Å, and  $c = 3.72$  Å, as shown in Fig. 1 [4]. The lattice parameters of the  $a$  and  $b$  axes are about twice as large as that of the  $c$  axis. Since the structure is an FCC derivative one, if atoms of the same type were placed on each site of this unit cell, it would become FCC structure. The (221) plane of the  $\text{Ni}_5\text{Al}_3$  is equivalent to the close-packed (111) plane of the FCC. Thus, the  $\text{Ni}_5\text{Al}_3$  (221) texture can be obtained right from the beginning of the  $\text{Ni}_5\text{Al}_3$  deposition since the  $\text{Ni}_5\text{Al}_3$  close-packed (221) planes have the lowest surface energy. Unlike the  $\text{NiAl}$  (112) texture, which is growth induced, a strong  $\text{Ni}_5\text{Al}_3$  (221) orientation is obtained by deposition from the start.

The  $\text{Ni}_5\text{Al}_3$  (221) planes have a small misfit with  $\text{CoCrPt}$  (10  $\bar{1}$  0) planes, as shown in Fig. 2. Consequently, a strong  $\text{Ni}_5\text{Al}_3$  (221) texture is expected to induce a strong  $\text{CoCrPt}$  (10  $\bar{1}$  0) texture by means of epitaxy.

## II. EXPERIMENTS

All the films discussed in this paper were deposited on Corning 7059 glass substrates at 25 °C by RF diode sputtering in a Leybold-Heraeus Z-400 system. The base pressure was  $5 \times 10^{-7}$  mtorr. The  $\text{CoCrPt}$  films were deposited with a fixed argon pressure of 10 mtorr, RF sputtering power of 2.3 W/cm<sup>2</sup>, and substrate bias voltage of -100 V. The composition of the  $\text{CoCrPt}$  thin films deposited at the substrate bias voltage

Manuscript received July 23, 2001; revised December 20, 2001. This work was supported by the Data Storage Systems Center at Carnegie Mellon University under Grant ECD-89-07068 from the National Science Foundation.

Y.-N. Hsu and D. E. Laughlin are with the Data Storage System Center, Carnegie Mellon University, Pittsburgh, PA 15213 USA.

D. N. Lambeth is with the Department of Electrical and Computer Engineering, Carnegie Mellon University, Pittsburgh, PA 15213 USA (e-mail: dl0p@ece.cmu.edu).

Publisher Item Identifier S 0018-9464(02)06372-0.

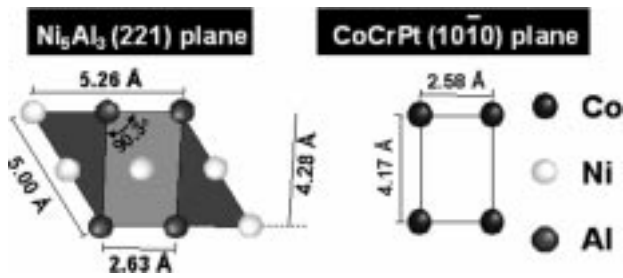


Fig. 2. Schematic of the lattice match of the  $\text{Ni}_5\text{Al}_3$  (221) and  $\text{CoCrPt}$  ( $10\bar{1}0$ ) planes.

of  $-100$  V was 78.5 at% Co, 9 at% Cr, and 12.5 at% Pt by inductively coupled plasma (ICP) analysis. The thicknesses of the  $\text{Ni}_5\text{Al}_3$  and  $\text{CoCrPt}$  films were fixed at 100 and 40 nm, respectively. *This CoCrPt thickness is greater than that used in current longitudinal recording media for the purpose of observing CoCrPt texture change.* The  $\text{Ni}_5\text{Al}_3$  films were deposited from either a  $\text{Ni}_1\text{Al}_1$  or a  $\text{Ni}_5\text{Al}_3$  target at 10 mtorr and  $2.3 \text{ W/cm}^2$ . If the  $\text{Ni}_1\text{Al}_1$  target was used, various substrate bias voltages were used in order to achieve the composition of  $\text{Ni}_5\text{Al}_3$ . The thickness of the  $\text{NiAl}$  thin films deposited with various substrate voltages were fixed at 100 and 400 nm. This is because the  $\text{NiAl}$  (112) texture is easily observed at the thick 400-nm  $\text{NiAl}$  thin film. The intermediate Cr and  $\text{NiAl}$  layers were deposited at a fixed argon pressure of 10 mtorr and RF sputtering power of  $2.3 \text{ W/cm}^2$ . The thicknesses of the intermediate Cr and  $\text{NiAl}$  layers were both fixed at 100 nm. Thin film texture characterization was carried out by using the Rigaku X-ray diffractometer (XRD) with  $\text{Cu } K\alpha$  radiation. A Philips EM 420 T transmission electron microscope (TEM) was used to observe microstructure. A vibrating sample magnetometer (VSM) with fields up to 10 kOe was used to measure magnetic properties.

### III. RESULTS AND DISCUSSIONS

#### A. $\text{Ni}_1\text{Al}_1$ Target With High Substrate Bias Voltage

Our initial attempts at making  $\text{Ni}_5\text{Al}_3$  underlayers were performed by using a  $\text{Ni}_1\text{Al}_1$  target with a substrate bias voltage applied. With no substrate bias voltage, XRD scans in Fig. 3(a) shows that the 100-nm  $\text{NiAl}$  thin film is (110) textured. For the 400-nm-thick  $\text{NiAl}$  thin film, both (110) and (112) peaks are observed in Fig. 3(b). If a low substrate bias voltage such as  $-100$  V is applied, a very strong  $\text{NiAl}$  (110) texture is obtained and the  $\text{NiAl}$  (112) texture disappears in both the 100- and 400-nm-thick films as shown in the XRD spectra (see Fig. 3). Substrate negative bias voltage attracts some positive argon ions to bombard the substrate surface. The atoms that are loosely bonded to neighboring atoms can be easily removed from the thin film by the bombarding argon ions. *Consequently, the crystallographic texture in the  $\text{NiAl}$  thin film shifts to a texture with closer packed plane if the substrate bias voltage is applied.* Since the  $\text{NiAl}$  (110) plane is the closest-packed plane for the B2 structure, (110) is expected to be the strongest XRD peak when the bias voltage of  $-100$  V is used. In addition, it is observed that the intensity of the  $\text{NiAl}$  (110) peak is strongest at a

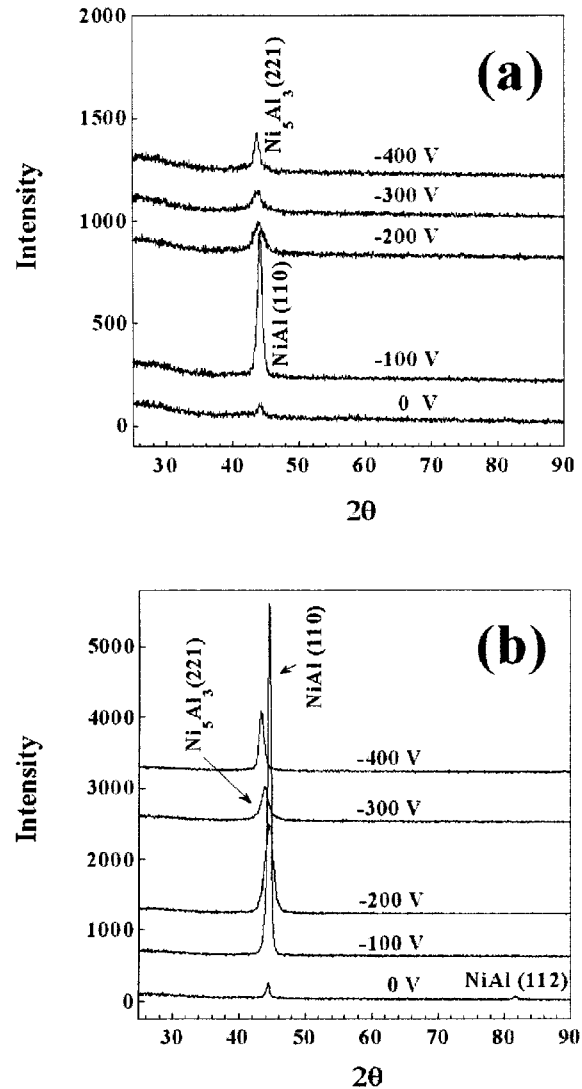


Fig. 3. X-ray diffraction spectra of the  $\text{NiAl}$  (a) 100-nm and (b) 400-nm thin films deposited with various substrate bias voltages.

substrate bias voltage of  $-100$  V and becomes weaker with increasing substrate bias voltages in Fig. 3(a) and (b). The position of this peak ( $2\theta$ ) also decreases about  $1^\circ$  in both XRD spectra of the 100- and 400-nm-thick  $\text{NiAl}$  films as the substrate bias voltage is increased to  $-300$  V. This peak position shift implies a lattice parameter change either due to the occurrence of a new phase, composition change, or stress resulting from the substrate bias voltage.

The electron diffraction pattern (EDP) of the 100-nm  $\text{NiAl}$  thin film at a substrate bias of  $-300$  V shows a ring pattern resulting from the  $\text{Ni}_5\text{Al}_3$  phase [Fig. 4(b)]. This pattern is different from the EDP of the B2 structure  $\text{NiAl}$  thin film obtained for the sample without substrate bias voltage applied [Fig. 4(a)]. *No  $\text{NiAl}$  ring was found in the  $\text{Ni}_5\text{Al}_3$  diffraction pattern shown in Fig. 4(b). This  $\text{Ni}_5\text{Al}_3$  (221) ring does not contain the  $\text{NiAl}$  (110) ring, although this ring appears to be thick.*

The  $\text{Ni}_5\text{Al}_3$  (221) X-ray diffraction peak position ( $2\theta$ ) is at  $43^\circ$ , which is  $1^\circ$  less than the  $\text{NiAl}$  (110) peak. The peak shift *as well as the weakening of the  $\text{NiAl}$  (110) peak at high substrate*

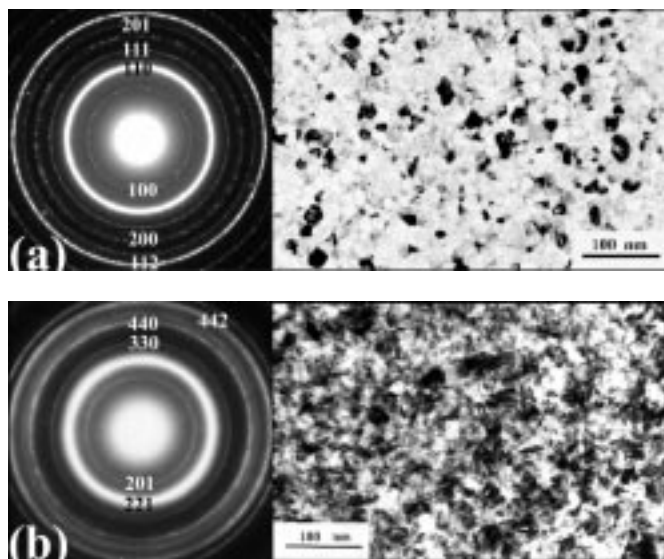


Fig. 4. TEM selected area diffraction and bright field image of the NiAl 100-nm thin film deposited with (a) 0 V and (b) –300 V substrate bias voltage. The TEM diffraction rings in Fig. 4(a) and (b) result only from NiAl and Ni<sub>5</sub>Al<sub>3</sub> phase, respectively.

*bias voltage* in the XRD spectra can be explained by the formation of the Ni<sub>5</sub>Al<sub>3</sub> phase at the bias voltages of –300 V. With substrate bias voltage applied, the Al atoms are more easily removed by the argon ion bombardment than the Ni atoms. Hence, we observed a Ni rich phase, i.e., Ni<sub>5</sub>Al<sub>3</sub>, to form.

The XRD spectra of the 40-nm CoCrPt–100-nm NiAl with various substrate bias voltages during NiAl deposition are shown in Fig. 5(a). The CoCrPt (10  $\bar{1}$  0) peaks are observed when the CoCrPt films are deposited onto the NiAl underlayers prepared at 0 and –300 V. As shown by the inserted XRD slow scan with 2 $\theta$  from 80° to 84° [Fig. 5(a)], the NiAl (112) texture is obtained only when no substrate bias voltage is applied. This NiAl (112) texture obtained at 0 V is observed to induce the CoCrPt (10  $\bar{1}$  0) texture. At the substrate bias voltage of –300 V, no NiAl (112) peak is observed in the XRD slow scan. Here, it is the Ni<sub>5</sub>Al<sub>3</sub> (221) texture that induces the CoCrPt (10  $\bar{1}$  0) texture due to the small misfit of the Ni<sub>5</sub>Al<sub>3</sub> (221) and CoCrPt (10  $\bar{1}$  0) planes, as shown in the CoCrPt and Ni<sub>5</sub>Al<sub>3</sub> epitaxial relationship in Fig. 2.

The magnetic properties of the 40-nm CoCrPt–100-nm NiAl thin films prepared with various substrate bias voltages are shown in Fig. 5(b). The coercivity and squareness are highest at zero bias voltage and decrease with increasing bias voltage due to the weakened NiAl (112) texture. The coercivity and squareness increase again at a bias voltage of –300 V because of the reappearance of the CoCrPt (10  $\bar{1}$  0) texture induced by the Ni<sub>5</sub>Al<sub>3</sub> (221) texture.

*B. Ni<sub>5</sub>Al<sub>3</sub> Alloy Target*

The EDP and bright field image of a 100-nm Ni<sub>5</sub>Al<sub>3</sub> thin film deposited from a Ni<sub>5</sub>Al<sub>3</sub> target are shown in Fig. 6(a) and (b), respectively. Due to the strong Ni<sub>5</sub>Al<sub>3</sub> (221) fiber texture, the (021), (440), and (442) reflections are observed in Fig. 6. In addition, the (221) rings are also observed, which indicates that

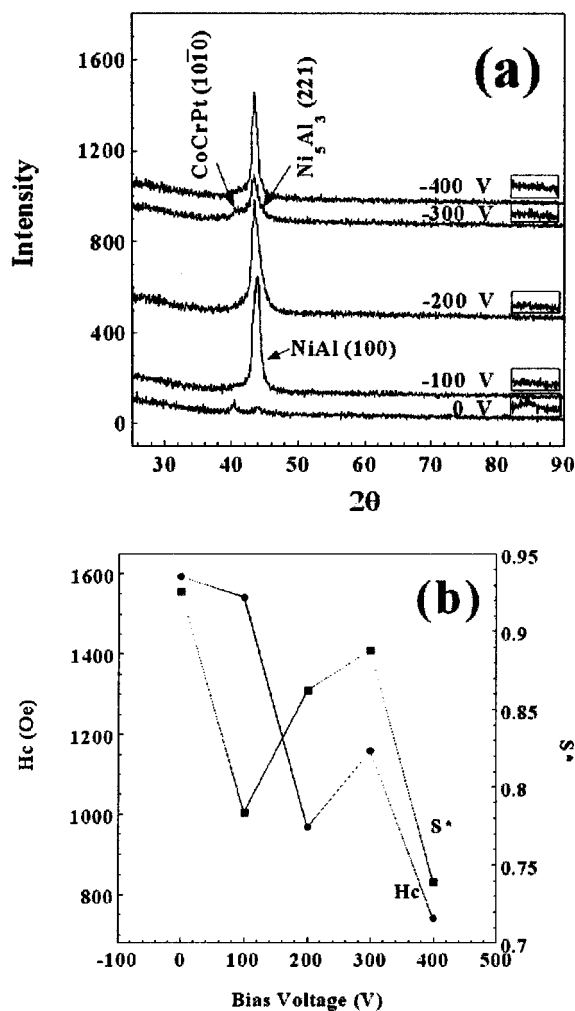


Fig. 5. (a) X-ray diffraction spectra and (b) magnetic properties of the 40-nm CoCrPt–100-nm NiAl thin films deposited with various substrate bias voltages.

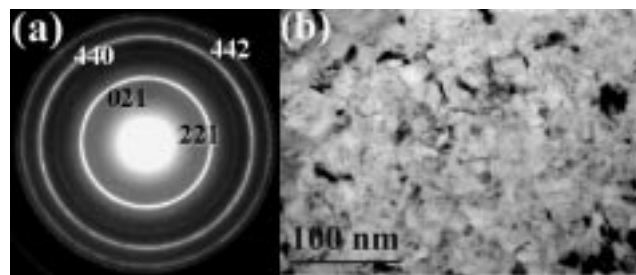


Fig. 6. TEM selected area diffraction and bright field image of the Ni<sub>5</sub>Al<sub>3</sub> 100-nm thin film directly deposited from the Ni<sub>5</sub>Al<sub>3</sub> alloy target.

some of the Ni<sub>5</sub>Al<sub>3</sub> grains are not (221) textured. The Ni<sub>5</sub>Al<sub>3</sub> grain size is about 10 nm.

The XRD spectra of the CoCrPt magnetic layer deposited onto the Ni<sub>5</sub>Al<sub>3</sub> underlayer directly from the Ni<sub>5</sub>Al<sub>3</sub> targets with the use of the Cr and NiAl intermediate layer are shown in Fig. 7(a). A strong Ni<sub>5</sub>Al<sub>3</sub> (221) peak is observed, consistent with the Ni<sub>5</sub>Al<sub>3</sub> (221) plane having the lowest surface energy. The CoCrPt (10  $\bar{1}$  0) peak is observed, indicating that the Ni<sub>5</sub>Al<sub>3</sub> texture induces the CoCrPt (10  $\bar{1}$  0) texture.

The in-plane magnetic properties of the films are shown in Fig. 7(b). Introducing a 100-nm Cr intermediate layer between

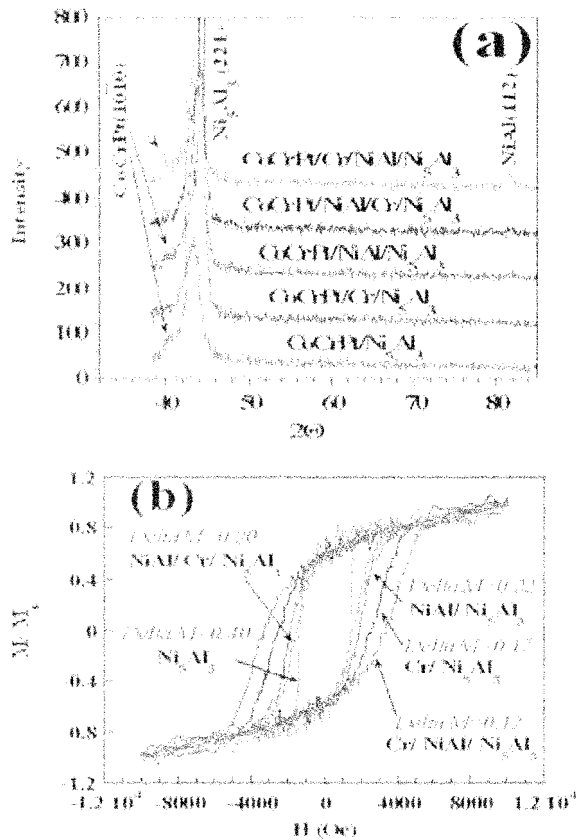


Fig. 7. (a) X-ray diffraction spectra and (b) magnetic properties of the CoCrPt 40-nm–Ni<sub>5</sub>Al<sub>3</sub> 100-nm thin films.

the CoCrPt and Ni<sub>5</sub>Al<sub>3</sub> layers decreases the CoCrPt (10  $\bar{1}$  0) peak intensity. However, the coercivity increases from 1440 to 2530 Oe. The peak  $\delta M$  value for the CoCrPt–Ni<sub>5</sub>Al<sub>3</sub> thin film is 0.4 and that of the CoCrPt–Cr–Ni<sub>5</sub>Al<sub>3</sub> thin film is 0.17. The exchange coupling is reduced by the Cr intermediate layer, which is most likely due to Cr diffusion from the intermediate layer to the CoCrPt grain boundaries [5]. The increase of the in-plane coercivity is mainly due to the reduction of the exchange coupling.

Adding a 100 nm NiAl film between the CoCrPt and Ni<sub>5</sub>Al<sub>3</sub> thin films can induce a NiAl (112) texture and hence an improved CoCrPt (10  $\bar{1}$  0) texture. The in-plane coercivity of the CoCrPt–NiAl–Ni<sub>5</sub>Al<sub>3</sub> thin film is about 1790 Oe. The coercivity of the CoCrPt–NiAl–Ni<sub>5</sub>Al<sub>3</sub> thin film is larger than that of the CoCrPt–Ni<sub>5</sub>Al<sub>3</sub> thin film due to an enhanced CoCrPt (10  $\bar{1}$  0) texture. The  $\delta M$  peak intensity is about 0.22, indicating stronger exchange coupling than that of the CoCrPt–Cr–Ni<sub>5</sub>Al<sub>3</sub> thin film.

TABLE I  
SUMMARY OF THE MAGNETIC PROPERTIES OF THE VARIOUS FILM STRUCTURES

Film structure	H <sub>c</sub> (Oe)	S*	Delta M
CoCrPt/Ni <sub>5</sub> Al <sub>3</sub>	1440	0.8419	0.40
CoCrPt/Cr/Ni <sub>5</sub> Al <sub>3</sub>	2530	0.4267	0.17
CoCrPt/NiAl/Ni <sub>5</sub> Al <sub>3</sub>	1790	0.5024	0.22
CoCrPt/NiAl/Cr/Ni <sub>5</sub> Al <sub>3</sub>	1650	0.4806	0.20
CoCrPt/Cr/NiAl/Ni <sub>5</sub> Al <sub>3</sub>	3380	0.5945	0.12

The CoCrPt–NiAl–Cr–Ni<sub>5</sub>Al<sub>3</sub> thin film does not show the CoCrPt (10  $\bar{1}$  0) and NiAl (112) peaks, indicating that the Cr layer does not grow epitaxially onto the Ni<sub>5</sub>Al<sub>3</sub> layer. The in-plane coercivity is about 1650 Oe and  $\delta M$  peak value is 0.2.

A CoCrPt–Cr–NiAl–Ni<sub>5</sub>Al<sub>3</sub> thin film shows strong CoCrPt (10  $\bar{1}$  0) and NiAl (112) peaks as seen in Fig. 7(a). This indicates that the Ni<sub>5</sub>Al<sub>3</sub> (221) texture can induce the NiAl (112) and CoCrPt (10  $\bar{1}$  0) texture. The in-plane coercivity is approximately 3380 Oe and  $\delta M$  is about 0.12. The high coercivity may be due not only to the good texture but also to the small exchange coupling as indicated by  $\delta M$  peak value. *The details of the magnetic properties of the various film structures discussed in this paper are listed in Table I.*

#### IV. CONCLUSION

We have shown that a Ni<sub>5</sub>Al<sub>3</sub> underlayer not only induces the CoCrPt (10  $\bar{1}$  0) texture, but also the NiAl (112) texture. The Ni<sub>5</sub>Al<sub>3</sub> improves the NiAl and CoCrPt texture and maintains a small grain size. Adding a Cr intermediate layer between the CoCrPt and Ni<sub>5</sub>Al<sub>3</sub> layers was shown to effectively reduce the media exchange coupling. This new media structure has the potential to yield a high coercivity and low noise magnetic recording media.

#### REFERENCES

- [1] L.-L. Lee, D. E. Laughlin, and D. N. Lambeth, "NiAl underlayers for CoCrTa magnetic thin films," *IEEE Trans. Magn.*, vol. 30, pp. 3951–3953, Nov. 1994.
- [2] D. E. Laughlin, B. Lu, Y.-N. Hsu, and D. N. Lambeth, "Microstructural and crystallographic aspects of thin film recording media," *IEEE Trans. Magn.*, vol. 36, pp. 48–53, Jan. 2000.
- [3] T. B. Massalski, *Binary Alloy Phase Diagrams*. Materials Park, OH: ASM Int., 1996.
- [4] P. Villars and L. D. Calvert, *Pearson's Handbook of Crystallographic-data for Intermetallic Phases*. Materials Park, OH: ASM Int., 1991.
- [5] Y. C. Feng, D. E. Laughlin, and D. N. Lambeth, "Interdiffusion and grain isolation in Co/Cr thin films," *IEEE Trans. Magn.*, vol. 30, pp. 3948–3950, Nov. 1994.